A Novel Modeling Concept for Multi-coupling Core Structures*

Pit-Leong Wong, Fred C. Lee, Xiaochuan Jia and Daan van Wyk

Center for Power Electronics Systems
The Bradley Department of Electrical and Computer Engineering
Virginia Polytechnic Institute and State University
Blacksburg, VA 24061 USA

Abstract - **Coupling inductors between two channels can improve both the steady state and dynamic performances of multi-channel interleaving voltage regulator modules (VRMs). However, the complicated electrical circuit model for the multi-coupling core structures prevents the coupling concept from being extended to integrated multi-channel core structures. This paper presents a novel circuit modeling concept that can be easily applied to different complicated multi-coupling core structures. Compared to conventional modeling methods, the proposed method involves fewer inductors. It is more directly related to the physical core structures and is easier to converge in computer simulation. Simulation results are presented to verify the validity of this modeling concept.**

I. Introduction

Multi-channel interleaving voltage regulator modules (VRMs) have been widely adopted as industry practice. With proper coupling design, the integration of the inductors in two of the interleaving channels with 180° phase shift improves both the steady-state performances and the transient responses [1]. The coupling effects reduce the steady-state current ripple and the equivalent transient inductance. The conduction losses in the MOSFETs can thus be reduced. The integrated coupling core structure also makes the fluxes more evenly distributed in the core, which reduces core losses. Experimental results show that the efficiency improvement due to the coupling core structure is significant. Moreover, the integrated coupling core structures make the manufacture of the cores easier and improve their mechanical stability.

For increasing current ratings of the VRMs, more interleaving channels become more desirable. Current research interest focuses on the use of integrated coupling core structures to improve the performance and increase the power density of multi-channel applications. However, the defects of existing electrical circuit modeling methods for complicated core structures prevent various studies of the different integrated coupling core structures. These defects include complexity, involving many inductors and controlled sources, converging problems in computer simulations, elements without clear physical meaning, and lack of scalabilities. This paper proposes a solution to these problems by presenting a novel electrical circuit modeling concept for the magnetic core structures. The proposed modeling concept uses minimum inductors and is easier to converge. The proposed modeling concept is closely related to the magnetic reluctance model, and the physical structure of the cores. The proposed modeling concept is easy to scale to different coupling channels.

II. Review of Existing Methods

The modeling of the integrated multi-channel core structures is similar to that of the multi-winding transformers, unless the leakage inductance in the transformers is much smaller than the magnetizing inductance. The leakage inductance in the transformers is actually the self-inductance in coupling inductor structures, while the common magnetizing inductance in transformers is the coupling inductance in coupling inductor structures. Modeling of the multi-winding transformer is an extensively researched area. This section reviews the existing common methods.

For two-winding transformers, the π-model is the most commonly used. The π-model can be easily simplified and applied in two-channel coupling inductor structures [1], as shown in Fig. 1. One extension of the π-model for three-channel coupling inductor structures is shown in Fig. 2. However, this model is not a general method. It is only valid for the special case in which the couplings among the channels are all the same. This cannot always be the case. As will be discussed later, some symmetric core structures may also result in different couplings among channels. The general mathematical model for multi-channel coupling inductor cases is described as Formula 1. There is a total of $n(n+1)/2$ independent components in the $n*n$ diagonal symmetric matrix. In order to describe the case generally, the circuit model needs to include $n(n-1)/2$ inductors in an n-channel coupling structure. A more general extension of the π-model for three-channel coupling inductor structures is given in Fig. 3 [3], which shows that this model is actually difficult to apply to coupling inductor structures because of the different definition of terminations and parameters in the model. Moreover, this model is also difficult to extend to more than three channels.

* This work made use of the ERC shared facilities supported by the National Science Foundation under award number EEC-9731677

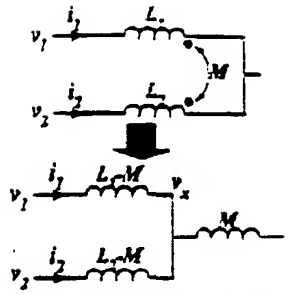

Fig. 1. Simplified π-model for two-channel coupling inductors.

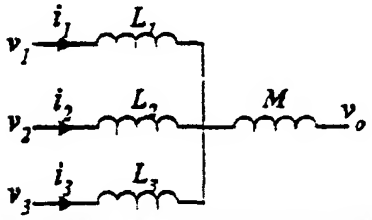

Fig. 2. A special extension of π-model for three-channel coupling inductors.

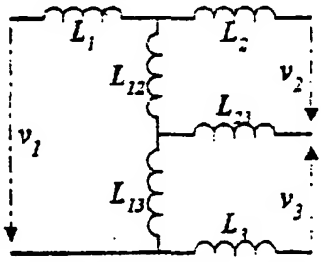

Fig. 3. A general extension of π-model for three-channel coupling inductors.

$$\begin{bmatrix} v_1 \\ v_2 \\ \vdots \\ v_n \end{bmatrix} = \begin{bmatrix} L_1 & L_{12} & \cdots & L_{1n} \\ L_{12} & L_2 & \cdots & L_{2n} \\ \vdots & \vdots & \ddots & \vdots \\ L_{1n} & L_{2n} & \cdots & L_n \end{bmatrix} \cdot \frac{d}{dt} \begin{bmatrix} i_1 \\ i_2 \\ \vdots \\ i_n \end{bmatrix} \qquad (1)$$

Considering the model shown in Fig. 1, the star connection of the three inductors can be replaced by the delta connection of the other three inductors with equivalent transformation, as shown in Fig. 4. The delta connection can be extended to multi-channel coupling structures. The delta connection modeling of a four-channel coupling structure is shown in Fig. 5 [4]. However, the inductors in the model are mathematical transformation results without clear physical meanings. The derivation and explanation of the parameters in the model are very difficult.

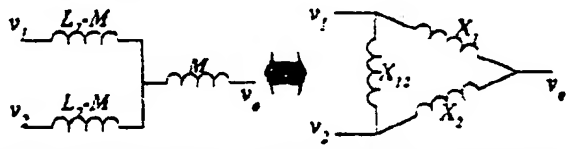

Fig. 4. Y-Δ transformation of π-model for two-channel coupling inductors.

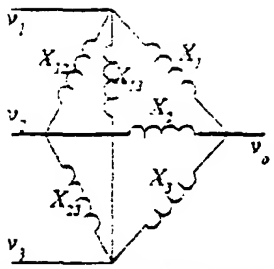

Fig. 5. Delta connection model for three-channel coupling inductors.

The general procedure to derive the electrical circuit model starts from the magnetic reluctance model. An example of a four-channel coupling inductor structure and its reluctance model are shown in Fig. 6. The magnetomotive force (MMF) sources, which are the products of the currents and turns of the windings, translate into voltage sources in the reluctance model to represent the windings, as shown in Fig. 6. The reluctance model, which can be easily derived from the core geometry and the material permeability, directly describes the core. The parameters in the model have clear physical meanings. However, this model cannot be directly used in circuit simulation to ascertain the electrical effect of the magnetic components. The reluctance model of the core needs to be transferred to the electrical model, which is the difficult part of the modeling. The major existing methods are as follows.

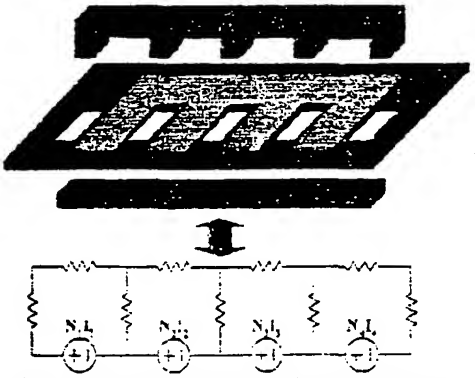

Fig. 6. Derivation of reluctance model from core structure.

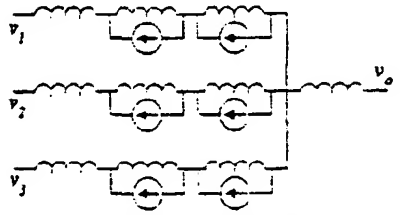

Fig. 7. A general modification of π-model for three-channel coupling core structure.

One method modifies the π-model shown in Fig. 2. The modification is shown in Fig. 7 [5]. The couplings between the windings are represented as the current sources and the inductance. A total of ten inductors and six controlled current sources are used for three-channel coupling inductors. This

model is apparently too complicated and its converging problems in computer simulation make it even more problematic.

Another method includes the magnetic reluctance model directly in the electric circuit simulation [6]. An interface between the magnetic and the electric circuit is necessary to transfer the parameters between the magnetic circuits and the electric circuits, as shown in Fig. 3. The interface relates the current and voltage in the electric circuit with the flux and MMF source in the magnetic reluctance model. Although the concept of the interface is simple, the implementation involves current-controlled current sources, current-controlled voltage sources, and inductors. The complexity of the interface results in time-consuming simulation and converging problems.

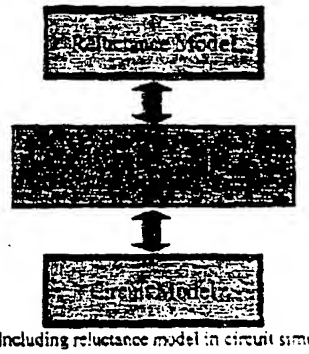

Fig. 3. Including reluctance model in circuit simulation.

The last method applies duality transformation rules to generate the electric model from the reluctance model [4, 6]. However, for complex core structures, the transformation is labor-intensive and has high probability of error. Since the model requires ideal transformers, it also has converging problems in circuit simulation.

The review of the existing modeling methods shows that they all have defects, such as complexity, converging problems in simulation, and difficulties in model derivation and explanation. In order to find a proper modeling method for multi-channel coupling inductor structures, this paper proposes a novel modeling method that starts from a different reluctance modeling concept.

III. Concept of The Proposed Method

In the magnetic reluctance model, the reluctances are only determined by core structure and material permeability. It is straightforward and cannot be changed. The windings are represented as the MMF sources, which are the currents that run through the windings. The existing modeling methods all use this method to derive the reluctance model.

From another point of view, the voltages applied to the windings are also the parameters that can represent the windings. According to Faraday's Law, the voltage applied to the winding integrated with the time (which is more simply stated as the voltage-second of the winding) determines the flux in the corresponding core leg, as shown in Formulas 2 and 3. The flux in the core is represented as the current in the reluctance model. Thus, the windings can also be represented as the current sources in the reluctance model. The values of the current sources are determined by the voltage-second of the windings. To distinguish this reluctance model from the conventional reluctance model, this one is named the flux source reluctance model while the conventional model is the MMF source reluctance model. The two models are equivalent. For the MMF source model, the MMFs are the known parameters, and the fluxes in the branches need to be determined. For the flux source model, the fluxes in the branches are the known parameters, and the MMFs of the loops need to be determined. Figure 9 is the flux source reluctance model for the core structure shown in Fig. 6. The only differences between the two reluctance models are the sources that represent the windings.

$$N \cdot \phi = \int V \cdot dt \tag{2}$$

$$V = N \cdot \frac{d\phi}{dt} \tag{3}$$

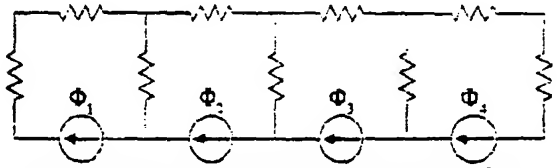

Fig. 9. Flux source reluctance model for the core structure in Fig. 6

For the flux source reluctance model, the MMF of a certain loop is determined by its reluctances and the fluxes through them. For the flux source reluctance model, the fluxes in the branches become very clear. The values can be easily gotten solely from observation. Accordingly, the MMF of each loop can also be determined easily. However, for the MMF source model, it is usually necessary to solve a set of n coupled equations in order to find out the branch fluxes in an n-channel coupling core structure. For the modeling methods shown in Fig. 3 and Fig. 5, solving the equation set is done by hand, which makes the parameters in the model difficult to derive and without clear physical meaning. For the other modeling methods reviewed in Section II, the equation set is solved in the circuit simulation, which makes the simulation time-consuming and causes convergence problems. In other words, the problems of the existing modeling methods are caused by the difficulty of solving the coupled equations.

The flux source reluctance model also requires solving a set of n equations, but the equations are decoupled. Solving n decoupled equations is much simpler than solving n coupled equations, especially when n increases. Although the flux source reluctance model and the MMF source reluctance model are equivalent, solving the flux source reluctance model is much simpler. This is the main reason that the circuit model based on the flux source reluctance model is much simpler than the circuit model based on the MMF source reluctance model.

For the model shown in Fig. 9, a general cell can be extracted, as shown in Fig. 10. According to Ampere's Law,

the MMF of Loop i, which represents the current in the winding, can be described in Formula 4. The formula can be very easily derived just by observing Fig. 10.

$$N_i \cdot i_i = (R_{i,i-1} + R_{i,i} + R_{i,i+1}) \cdot \phi_i - R_{i,i-1} \cdot \phi_{i-1} - R_{i,i+1} \cdot \phi_{i+1} \quad (4)$$

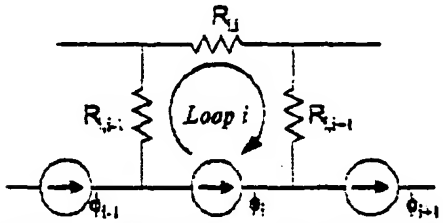

Fig. 10. A general cell in the flux source reluctance model.

The sum of the reluctances in Loop i, $R_i = \sum_j R_{i,j} = (R_{i,i-1} + R_{i,i} + R_{i,i-1})$, is defined as the self-reluctance of Loop i. The reluctance involving both Loop i and j, $R_{i,j}$, is defined as the mutual reluctance between these two loops. As shown in Formula 4, the MMF can be divided into two parts: the self-MMF, which is generated by flux ϕ_i through the self-reluctance of the loop, and the mutual MMF, which is generated by fluxes other than ϕ_i through the corresponding mutual-reluctances.

Formula 5 is the differentiation of Formula 4. Submitting Formula 3 into Formula 5 results in Formula 6. Formula 6 represents the current through the corresponding winding.

$$N_i \cdot \frac{d}{dt} i_i = R_i \cdot \frac{d}{dt} \phi_i - R_{i,i-1} \cdot \frac{d}{dt} \phi_{i-1} - R_{i,i+1} \cdot \frac{d}{dt} \phi_{i+1} \quad (5)$$

$$\frac{di_i}{dt} = \frac{R_i}{N_i^2} \cdot v_i - \frac{R_{i,i-1}}{N_i \cdot N_{i-1}} \cdot v_{i-1} - \frac{R_{i,i+1}}{N_i \cdot N_{i+1}} \cdot v_{i+1} \quad (6)$$

The definition of the inductances is shown in Formula 7. The inductance $L_{i,i}$ is defined as the self-inductance of Loop i, which corresponds to the self-reluctance of the loop. The inductance $L_{i,j}$ is defined as the mutual inductance between Loop i and j, which corresponds to the mutual reluctance between the two loops. All these inductances have clear physical meanings, and are closely related to the magnetic core structure.

$$\begin{cases} L_{i,i} = \dfrac{N_i^2}{\sum_j R_{i,j}} & self-inductance \\ L_{i,j} = -\dfrac{N_i \cdot N_j}{R_{i,j}} & mutual-inductance \end{cases} \quad (7)$$

With the definitions in Formula 7, Formula 6 can be simplified into Formula 8.

$$\frac{di_i}{dt} = \frac{1}{L_{i,i}} \cdot v_i + \frac{1}{L_{i,i-1}} \cdot v_{i-1} + \frac{1}{L_{i,i+1}} \cdot v_{i+1} \quad (8)$$

The current through a winding can be divided into two parts: the self-current, which is the first item in Formula 8, and the mutual (or coupling) currents, which is the rest of the items in Formula 8. The definitions of self-current and mutual current are shown in Formula 9. Formula 8 can be rewritten as Formulas 10 and 11.

$$\begin{cases} i_{i,i} = \dfrac{\int v_i \cdot dt}{L_{i,i}} & self-current \\ i_{i,j} = \dfrac{\int v_j \cdot dt}{L_{i,j}} & mutual-current \end{cases} \quad (9)$$

$$\frac{di_i}{dt} = \frac{d}{dt} i_{i,i} + \sum_j \frac{d}{dt} i_{i,j} \quad (10)$$

$$i_i = i_{i,i} + \sum_j i_{i,j} \quad (11)$$

The voltage applied to the winding and the self-inductance determine the self-current through the winding. The voltage on the other windings and the corresponding mutual inductances determine the mutual currents. The self-current is the decoupled part of the winding current. The mutual currents are the coupling effects among different windings. In this specific case, the mutual currents have only two parts, which correspond to the two adjacent windings. In physical reality, there are coupling effects among all the windings. This model has simpler expression, but the coupling effects remain. As it is shown in Section IV, this model does result in the coupling of all the windings, as do the other models.

The total current through a winding is generated by several winding voltages. In other words, the voltage applied to a certain winding not only generates the self-current in the winding, but also generates the mutual currents in the other windings. The mutual and self-currents generated by the same voltage have waveforms proportional to each other. The mutual-current waveforms can be described as the self-current waveform generated by the same voltage with a proportional coefficient. Another format of Formula 9 is shown in Formula 12. The coefficient between the mutual and self-currents generated by the same voltage can be found by comparing the two equations in Formula 12. The result is shown in Formula 13. The coefficients $\alpha_{i,j}$ are only determined by the reluctances. As previously discussed, the parameters are directly related to the core structure, can be easily derived, and have clear physical meanings.

$$\begin{cases} i_{i,i} = \dfrac{\int v_i \cdot dt}{L_{i,i}} \\ i_{i,j} = \dfrac{\int v_j \cdot dt}{L_{i,j}} \end{cases} \quad (12)$$

$$\alpha_{i,j} = \frac{i_{i,i}}{i_{j,j}} = \frac{L_{i,j}}{L_{i,i}} = \frac{R_{i,j}}{R_i} = \frac{R_{i,j}}{\sum_j R_{j,j}} \quad (13)$$

With Formula 13, Formula 11 can be rewritten as Formula 14.

$$i_i = i_{i,i} + \sum_j \alpha_{i,j} \cdot i_{j,j} \tag{14}$$

The matrix format of Formula 14 is shown in Formula 15. The total currents in the windings can be represented as the linear transformation of the self-currents in the windings. Matrix A in Formula 15 represents the linear transformation.

$$\begin{bmatrix} i_1 \\ i_2 \\ \vdots \\ i_n \end{bmatrix} = \begin{bmatrix} 1 & \alpha_{1,2} & \cdots & \alpha_{1,n} \\ \alpha_{2,1} & 1 & \cdots & \alpha_{2,n} \\ \vdots & \vdots & \ddots & \vdots \\ \alpha_{n,1} & \alpha_{2,n} & \cdots & 1 \end{bmatrix} \cdot \begin{bmatrix} i_{1,1} \\ i_{2,2} \\ \vdots \\ i_{n,n} \end{bmatrix} = A \cdot \begin{bmatrix} i_{1,1} \\ i_{2,2} \\ \vdots \\ i_{n,n} \end{bmatrix} \tag{15}$$

As discussed previously, the self-current in a winding is the decoupled part of the winding current. It is determined only by the corresponding individual winding voltage. Formula 15 can be further written as Formula 16. Formula 16 is a general expression of the results of the flux source reluctance model for n-channel coupling magnetic structures. For known voltage sources applied to the corresponding windings, Formula 16 gives the current waveform in the winding. The required parameters in Formula 16 are the coefficients of matrix A and the self-inductances $L_{i,i}$. As discussed, all the parameters in the formula can be derived directly from the reluctance model solely by observation. The results can be reached by a simple matrix multiplication avoiding problematic solving of n-coupled equations encountered in conventional modeling methods. Thus, this method is much simpler.

$$\begin{bmatrix} i_1 \\ i_2 \\ \vdots \\ i_n \end{bmatrix} = A \cdot \begin{bmatrix} i_{1,1} \\ i_{2,2} \\ \vdots \\ i_{n,n} \end{bmatrix} = A \cdot \begin{bmatrix} \dfrac{\int v_1 \cdot dt}{L_{1,1}} \\ \dfrac{\int v_2 \cdot dt}{L_{2,2}} \\ \vdots \\ \dfrac{\int v_n \cdot dt}{L_{n,n}} \end{bmatrix} \tag{16}$$

From another point of view, Formula 1 is the general expression of the results of the MMF source reluctance model. Formula 6 is just the inverse transformation of Formula 1. Matrix A in Formula 16 is the inversive matrix of the inductance matrix in Formula 1. The elements of Matrix A in Formula 16 are directly related to the reluctance model with clear physical meanings, while the elements of the inductance matrix in Formula 1 cannot be easily related to the reluctance model. To derive the parameters in Formula 1, matrix inversion is unavoidable. Matrix inversion is actually the solving of the linear equation set mentioned previously. The current source reluctance model avoids matrix inversion, thus reducing the complexity.

The next step is to implement the model in circuit simulation. From Formula 16, the model requires n independent inductors for n-channel coupled core structures. The elements in Matrix A, $\alpha_{i,j}$, can be represented by the controlled current sources. The simulation model for the general cell shown in Fig. 10 and Formula 6 is shown in Fig. 11. The function of the controlled current sources in Fig. 11 is to add up the currents in the different inductors. They are not involved in circuit simulation as they are in the model of Fig. 7. Thus, the proposed method does not have converging problem seen in the conventional methods' simulations.

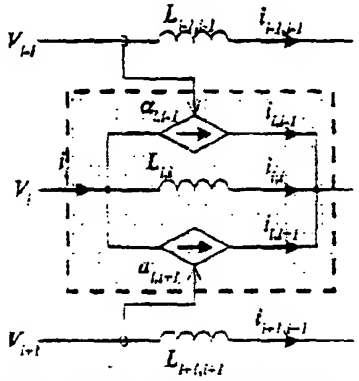

Fig. 11. Simulation model for the general cell.

IV. Verification and Simulation Results of the Proposed Model

In order to verify the validity of the proposed modeling method, simulation circuits with coupling core structures are built based on both the proposed model and the conventional models. The circuit is an n-channel interleaving quasi-square-wave (QSW) converter with coupling core structures and is shown in Fig. 12. As mentioned previously, for two-channel coupling core structures, the conventional magnetic modeling (shown in Fig. 1) is sufficiently accurate and fast. For two-channel coupling core structures, the proposed magnetic model will compare with the model shown in Fig. 1.

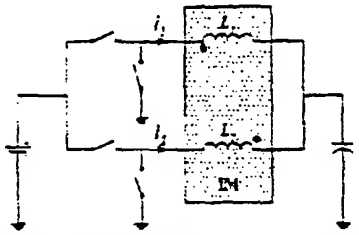

Fig. 12. Interleaving QSW converter with coupling core structures for simulation.

The simulation results of the winding current for both models are shown in Fig. 13 by replacing the shaded area in Fig. 12 with the model shown in Fig. 1 and 11. The two modeling methods give exactly the same results.

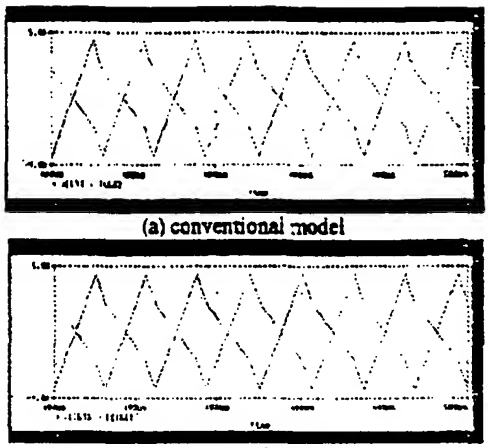

(a) conventional model

(b) proposed model

Fig. 13. Simulation results for two-channel interleaving QSW converter with coupling core structures.

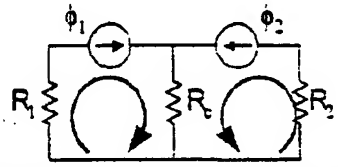

Fig. 14. Reluctance model of a two-channel coupling core structures.

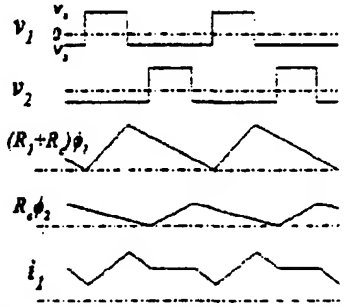

Fig. 15. Analysis of the waveforms in the proposed method.

For the integrated magnetic core structure shown in [1], the reluctance model of the core is shown in Fig. 14. As illustrated in Formula 6, the proposed magnetic model is actually a weighted sum of the different voltage-seconds applied to the integrated magnetic core. To explain the concept more clearly, the process is illustrated in Fig. 15. For the two-channel interleaving QSW converters, the voltage waveforms applied to the two windings are the waveforms of v1 and v2 shown in Fig. 15. The integration of the waveforms gives the flux waveforms in the corresponding core legs. The flux waveforms with the weighted coefficient are the waveforms of $(R_1 + R_c)\cdot\phi_1$ and $R_c\cdot\phi_2$ in Fig. 15. The current waveform in the winding, which is the waveform of i1 in Fig. 15, is just the sum of the flux waveforms of ϕ_1 and ϕ_2 with weighted coefficients of $(R_1 + R_c)$ and R_c, respectively. The flux waveforms are actually proportional to the self-current waveforms, which are also the currents through the self-inductors in Fig. 11. The controlled current sources in the proposed model (as shown in Fig. 11) are just to get the weighted sum of the flux waveforms. The winding current can be easily gotten using the proposed method. Thus, there is no converging problem in thecircuit simulation.

The channel current simulation results for three-channel coupling core structures for the conventional model and the proposed model are compared in Fig. 16. The two simulation results are exactly the same. These simulation results confirm the validity of the proposed model for coupling core structures.

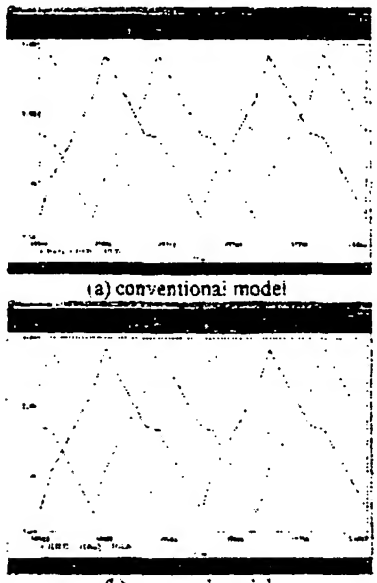

(a) conventional model

(b) proposed model

Fig. 16. Simulation results for three-channel interleaving QSW converter with coupling core structures.

As mentioned previously, the purpose of this model is to be able to be applied to more complicated coupling core structures in order to identify the performances of different core coupling structures. Figure 17 gives the simulation current waveforms of the four-channel integrated coupling core structure shown in Fig. 6 with a certain winding arrangement. The detail performance evaluations of the different coupling core structures are beyond the scope of this paper. The purpose of this paper is to show that the proposed magnetic model can easily handle a variety of complicated coupling core structures.

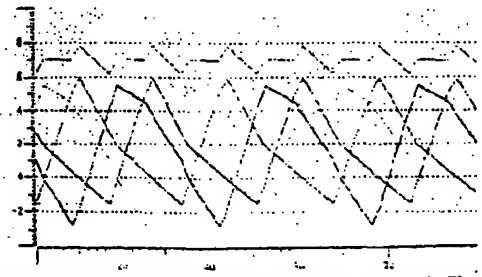

Fig. 17. Simulation results for the coupling core structure in Fig. 6.

For the specific core structure shown in Fig. 6, Matrix A in Formula 16 has the following format.

$$A=\begin{bmatrix} L_{11}^{-1} & L_{12}^{-1} & 0 & 0 \\ L_{21}^{-1} & L_{22}^{-1} & L_{23}^{-1} & 0 \\ 0 & L_{32}^{-1} & L_{33}^{-1} & L_{34}^{-1} \\ 0 & 0 & L_{43}^{-1} & L_{44}^{-1} \end{bmatrix} \qquad (17)$$

From the viewpoint of the flux source modeling, the fluxes are only affected by the self and the two adjacent voltage sources. That is the reason for the zeros in the matrix. Of course, in reality all the windings are coupled. The flux source modeling does not change the fact but simplifies the model.

The inductance matrix for the conventional magnetic modeling in Formula 1 is the inversion of Matrix A, which could be overwhelmingly complicated. For simplification, assume that all the mutual inductances in Formula 17 are the same as M. The inversion of Matrix A is shown in Formula 18. It is much more complicated than Formula 17. This implies that the proposed flux source magnetic modeling method gives much simpler simulation models for multi-channel coupling core structures. From Formula 18, it is also clear that all the four inductors are coupled. Although the coupling is not explicitly shown in Formula 16, the two formulas describe the same fact. The simulation waveforms and the formulas also show that the seemingly symmetric core structure actually gives an asymmetric coupling pattern. Only with the accuracy and simplicity of the proposed magnetic modeling concept can the analysis of these subtle performance differences become possible.

$$A^{-1}=\frac{1}{\left(M^4-3\cdot L^2\cdot M^2+L^4\right)}\cdot L^4\cdot M^4\cdot\begin{bmatrix} \frac{\left(M^2-2\cdot L^2\right)}{\left(L^3\cdot M^2\right)} & \frac{-1}{M^3}\frac{\left(M^2-L^2\right)}{L^2} & \frac{1}{\left(M^2\cdot L\right)} & \frac{-1}{M^3} \\ \frac{-1}{M^3}\frac{\left(M^2-L^2\right)}{L^2} & \frac{1}{L^3}\frac{\left(M^2-L^2\right)}{M^2} & \frac{-1}{\left(L^2\cdot M\right)} & \frac{1}{\left(M^2\cdot L\right)} \\ \frac{1}{\left(M^2\cdot L\right)} & \frac{-1}{\left(L^2\cdot M\right)} & \frac{1}{L^3}\frac{\left(M^2-L^2\right)}{M^2} & \frac{-1}{M^3}\frac{\left(M^2-L^2\right)}{L^2} \\ \frac{-1}{M^3} & \frac{1}{\left(M^2\cdot L\right)} & \frac{-1}{M^3}\frac{\left(M^2-L^2\right)}{L^2} & \frac{\left(M^2-2\cdot L^2\right)}{\left(L^3\cdot M^2\right)} \end{bmatrix} \qquad (18)$$

V. Conclusion

The conventional magnetic modeling methods are too complicated to be useful for multi-channel coupling core structures. This paper presents a novel flux source modeling concept for the magnetic modeling of multi-channel coupling core structures. The method is much simpler than the conventional methods. Moreover, the proposed method is directly related to the magnetic reluctance model. Every element in the model has clear physical meanings. Circuit simulation results for both methods are compared to verify the validity of the proposed method. An example of a four-channel coupling core structure is provided to show the great reduction of complexity achieved by the proposed modeling method compared to the conventional methods.

The proposed magnetic modeling method is suitable to evaluate the performances of the different multi-channel coupling core structures.

References

[1] P. Wong, P. Xu, B. Yang and F. C. Lee, "Performance Improvements of Interleaving VRMs with Coupling Inductors," *CPES Annual Seminar*, 2000, pp. 317-324.

[2] P. Wong, Q. Wu, P. Xu, B. Yang and F. C. Lee, "Investigating Coupling Inductor in Interleaving QSW VRM," *IEEE APEC*, 2000. pp. 973-978.

[3] Alexander S. Langsdorf, *Theory of Alternating-Current Machinery*, pp. 239-245.

[4] A. Dauhajre and R. D. Middlebrook, "Modeling and Estimation of Leakage Phenomena in Magnetic Circuits," *IEEE PESC*, 1986, pp. 213-226.

[5] Q. Chen, F. C. Lee, J. Jiang and M. M. Jovanovic, "A New Model for Multiple-Winding Transformer," *IEEE PESC*, 1994, pp. 864-871.

[6] S. A. El-Hamamsy and Eric Chang, "Magnetics Modeling for Computer-Aided Design of Power Electronics Circuits," *IEEE PESC*, 1989, pp. 635-645.